LIST OF ACRONYMS AND SYMBOLS

ACRONYMS

Acronym	Definition
DEC	Digital Equipment Corporation
EDU	Experimental Diving Unit
EVA	Extra-vehicular activity
FSW	Feet of sea water
HELIOX	Helium-oxygen
M-Values	Maximum allowed tissue tensions
RNPL	Royal Naval Physiological Laboratory
SCUBA	Self-contained underwater breathing apparatus
USN	United States Navy
VP	Varying permeability
VPM	Varying-permeability model

SYMBOLS

Symbol	Definition
a, A	Algebraic intermediate variables
b, B	" " "
c, C	" " "
D	Depth
D_a	Allowed depth
F	Inert-gas fraction
F_{He}	Helium inert-gas fraction
H	Tissue half-time

LIST OF ACRONYMS AND SYMBOLS (CONTINUED)

Symbol	Definition
H^*	Tissue exponential time-constant
k	Inverse of tissue exponential time-constant
N_{actual}	Actual bubble number
N_{new}	Augmented bubble number
N_o	Bubble number normalization constant
N_{safe}	Safe bubble number
p	Algebraic intermediate variable
P^*	Crushing pressure threshold
P_a	Ambient pressure
P_{crush}	Permeable region crushing pressure
P^*_{crush}	Impermeable region crushing pressure
P_f	Final pressure
P_{in}	Pressure inside bubble nucleus
P_m	Maximum pressure
P_o	Initial ambient pressure
P_R	Pressure outside nucleus, including surface tension
P_S	Pressure inside nucleus, including skin compression
P_{ss}	Allowed supersaturation pressure
P^{new}_{ss}	Augmented allowed supersaturation pressure
P^{safe}_{ss}	Safe, unaugmented allowed supersaturation pressure
P_1	Exposure pressure
P_2	Final pressure
q	Algebraic intermediate variable

preliminary relationship between the model equations and the allowed tissue supersaturation. In Chapter II, several equations which supplement the decompression criterion are developed: the allowed supersaturation is augmented by the dynamic critical-volume hypothesis, a perfusion-limited equation is used to describe the exponential uptake and elimination of gas by the controlling tissue, and the regeneration of crushed nuclei is considered.

C. THE MODEL EQUATIONS

During a rapid compression from an initial ambient pressure P_o to some increased pressure P_m (Fig. 1), each included bubble nucleus is subjected to a "crushing" effect which decreases its radial size. This results in an increased tolerance to supersaturation since smaller nuclei will form macroscopic bubbles less readily than larger ones. The greater the crushing pressure P_{crush}, the greater the supersaturation required to form a given number of harmful bubbles. There is another way to characterize the data: for any pressure schedule, all nuclei which are initially larger than some "critical" radius r_o will grow to form macroscopic bubbles, while the rest will not.

The first of the varying-permeability model equations relates the crushing pressure P_{crush} to the corresponding change in the critical radius from r_o to r_m. At the onset of decompression, r_m characterizes the smallest nucleus which will produce a macroscopic bubble, just as r_o did prior to crushing. For the permeable compression from P_o to P_m, we have [10]

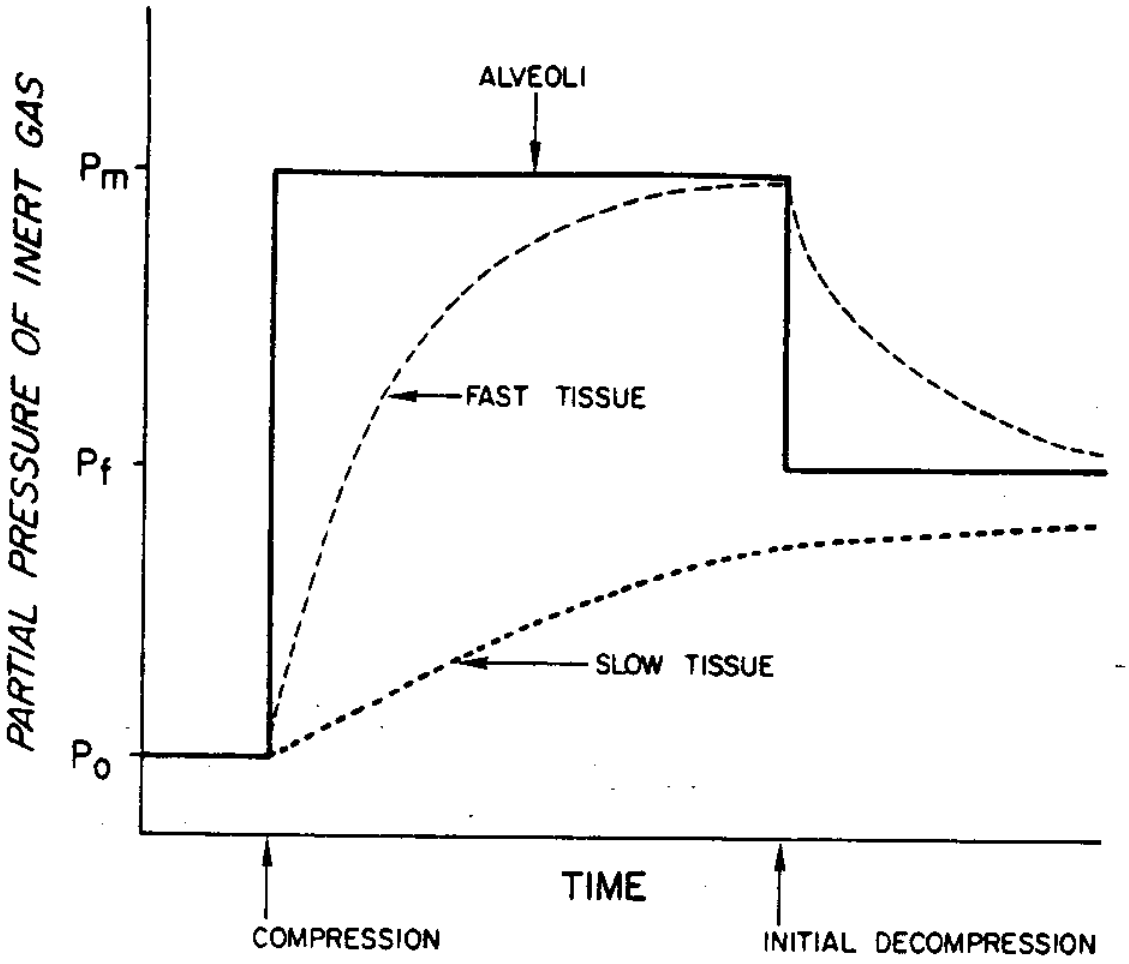

Fig. 1 - Response of fast and slow tissues exposed to a rectangular pressure schedule consisting of a rapid compression from an initial pressure P_o to some maximum pressure P_m and a rapid decompression to an intermediate pressure P_f.

$$P_{crush} = P_m - P_o = 2(\gamma_C - \gamma)(1/r_m - 1/r_o) \quad , \tag{1.1}$$

where γ is the surface tension and γ_c is the "crumbling" or maximum compressional strength of the surfactant skin. When P_m exceeds the changeover point P^* (9.2 atm abs), the equation appropriate to the impermeable region must be used, and for the impermeable compression from P^* to P_m, we have [10]

$$P^*_{crush} = P_m - P^* = 2(\gamma_C - \gamma)(1/r_m - 1/r^*) + P^* + 2P_o + P_o(r^*/r_m)^3, \tag{1.2}$$

where

$$r^* = [(P^*-P_o)/2(\gamma_C-\gamma) + 1/r_o]^{-1} \tag{1.3}$$

is the radius of the critical nucleus at the onset of impermeability, found by replacing P_m and r_m with P^* and r^* in Eq. (1.1).

The allowed supersaturation is given by [7]

$$P_{ss} = P_m - P_f = 2(\gamma/\gamma_C)(\gamma_C - \gamma)/r_m \quad , \tag{1.4}$$

which can be solved by rearranging Eqs. (1.1) and (1.2) to obtain values for r_m. The result is

$$r_m = [P_{crush}/2(\gamma_C-\gamma) + 1/r_o]^{-1} \tag{1.5}$$

for the permeable regime, while for the impermeable regime one must solve the cubic equation,

$$r_m^3 - 2(\gamma_C-\gamma)r_m^2 - (P_o/c)r^{*3} = 0 \tag{1.6}$$

with

$$c = P^*_{crush} - P^* + 2P_o + 2(\gamma_C-\gamma)/r^* \quad . \tag{1.7}$$

The solution is found in standard mathematical tables:

$$p = -2(\gamma_c - \gamma)/c \quad , \tag{1.8}$$

$$q = -P_o r^{*3}/c \quad , \tag{1.9}$$

$$a = -p^2/3 \quad , \tag{1.10}$$

$$b = (2/27)p^3 + q \quad , \tag{1.11}$$

$$A = [-b/2 + (b^2/4 + a^3/27)^{1/2}]^{1/3} \quad , \tag{1.12}$$

$$B = [-b/2 - (b^2/4 + a^3/27)^{1/2}]^{1/3} \quad , \tag{1.13}$$

$$r_m = A + B - p/3 \quad . \tag{1.14}$$

The cubic equation has two additional roots, but it can be shown that they are always negative or imaginary, given realistic values for the model parameters. To attempt a more explicit solution for r_m is impractical, thus the above equations have been inserted directly into the computer program.

It has been shown that the allowed supersaturation can be found for any rectangular pressure schedule by specifying only three parameters: γ, γ_c, and r_o. In addition, it is a feature of the model that the supersaturation is dependent only upon the ratios γ/γ_c and γ/r_o. Thus there is some flexibility afforded in selecting absolute values for γ, γ_c, and r_o. Also, by specifying the given ratios instead, the number of free parameters can be reduced from three to two. As will be shown, the critical-volume hypothesis and nuclear regeneration require one free parameter each, for a total of four.

CHAPTER II

A. THE CRITICAL-VOLUME HYPOTHESIS

In previous applications of the varying-permeability model [11,12], the number of macroscopic bubbles evolved during decompression was used to quantify decompression stress. Schedules which produced the same number of bubbles were assumed to cause the same decompression liability. This method worked remarkably well for rudimentary schedules and outcomes, such as pressure excursion limits and injury versus no-injury situations. The first VPM tables (unpublished) were thus based on the assumption that the body could accommodate a certain number of bubbles. The bubble number was equal to the number of nuclei initially present with radii larger than some critical radius r_o, and the allowed supersaturation was calculated using Eq. (1.4). This method generated schedules th were quite reasonable for lengthy dives but failed in the case of sho r dives, where it required excessive decompression times. In particular, satisfactory no-stop limits could not be produced concurrently with saturation dive schedules using the same nucleation parameters. The no-stops were "too safe" because the bubble number was being limited by the saturation dives.

It is known that tables currently in use often allow many bubbles to form during decompression. These can be detected by Doppler monitoring [26]. Apparently, the body can support some bubbles without outward signs of decompression stress. Of course, the long-term effects of repeated exposure to such bubble formation remain undefined and, perhaps, unsuspected. Among the many possible scenarios are an

increased incidence of osteonecrosis and "punch-drunk" behavior in divers, attributable to the chronic random destruction of cells in brain and bone. The incidence of macroscopic bubble formation in human blood or tissue can no longer be ignored in the creation of decompression tables: merely avoiding the bends may not guarantee diver safety.

The "primary" bubbles formed directly from nuclei may lead to "secondary" bubbles via fission [27] in blood or by the creation of "rosaries" in the interstitial spaces of the firmer tissues [28]. Since tissue deformation and impairment of circulation should depend upon both the size and the number of bubbles, it seems plausible that the total volume of evolved gas would serve as an effective criterion [29]. This would permit the formation of many small bubbles or of very few large ones. The "constant-bubble-number" hypothesis has thus been replaced by the "critical-volume" hypothesis and the number of bubbles has been allowed to fluctuate accordingly. For shorter total decompression times, bubble nuclei have little time during which to inflate. The permissible critical radius is then smaller and the allowed supersaturation larger, resulting in many small bubbles. Conversely, during long decompressions, bubbles may grow very large, so only a few are permitted. Because the number density and size distribution of nuclei *in vivo* are unknown, the table calculations are based upon an iterative procedure which does not explicitly determine the number of bubbles or the volume of released gas.

The original safe-ascent criterion was based on Eq. (1.4) and gave lines of constant bubble number (Fig. 2) [6] which were associated with lines of constant decompression stress. Our latest revision alters that

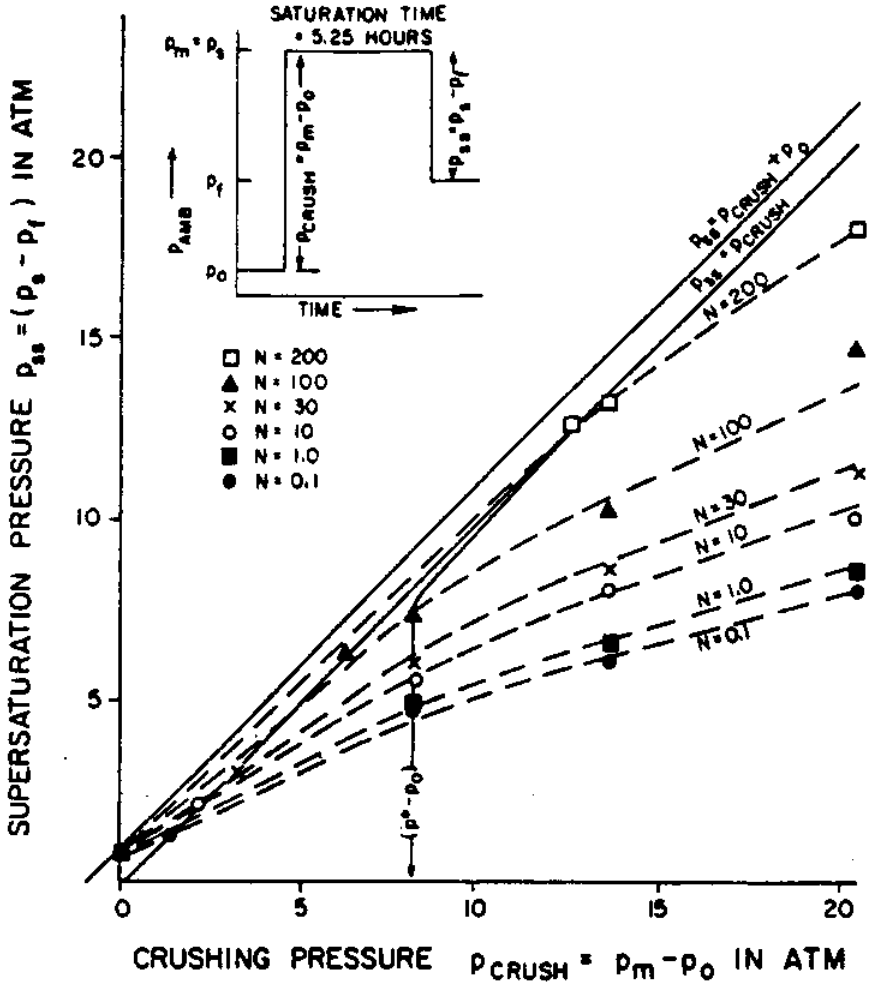

Fig. 2 - Plot of supersaturation versus crushing pressure for various lines of constant bubble number. The sudden decrease in slope at P_{crush} = 8.2 atm indicates the onset of impermeability.

criterion by augmenting the allowed supersaturation. This is accomplished by permitting the gas phase to inflate during decompression, under the constraint that the total volume of free gas never exceeds some critical value V_C. The rate at which the gas phase inflates is assumed to be proportional both to the number of bubbles in excess of the safe-ascent criterion and to the new supersaturation,

$$P_{ss}^{new}(t)(N_{new} - N_{safe}) = \chi \dot{V} \quad , \tag{2.1}$$

where χ is the constant of proportionality. The total volume of released gas must remain below V_C and can be found by integrating Eq. (2.1),

$$\int_o^t P_{ss}^{new}(t)(N_{new} - N_{safe})dt = \chi V_C \ . \tag{2.2}$$

In this case, the integral must reach its maximum value at time t_C so as not to exceed the volume V_C. Since the bubble numbers are constant after the first decompression step, they are independent of time. The new decompression criterion is then

$$(N_{new} - N_{safe}) \int_o^{t_C} P_{ss}^{new}(t)\, dt = \chi V_C \ . \tag{2.3}$$

Adopting a form for P_{ss}^{new} which is positive definite and letting the time t_C go to infinity is one way to guarantee that the integral is maximized. It is therefore assumed that P_{ss}^{new} remains constant during the decompression time t_D and decays exponentially thereafter. In practice, the supersaturation will eventually become slightly negative, since humans equilibrated at atmospheric pressure are inherently unsaturated by some 54 mm Hg [30]. Unfortunately, the time at which the integral would reach its maximum under those conditions is unknown. The

assumed form of P_{ss}^{new} is conservative, since the true value will be a little lower, and the net volume of free gas will be somewhat less than V_C. The integral and its solution are

$$(N_{new} - N_{safe})\{\int_o^{t_D} P_{ss}^{new}\, dt + \int_{t_D}^{\infty} P_{ss}^{new} \exp[(t_D-t)/H^*]dt\} ,$$

$$= (N_{new} - N_{safe})\, P_{ss}^{new}\, (t_D + H^*) = \chi V_C , \qquad (2$$

where P_{ss}^{new} is now a constant, $H^* = H/\ln 2$ is the exponential time constant, and H is the half-time of the controlling tissue.

The new supersaturation criterion is thus

$$P_{ss}^{new} = \chi V_C \,/\, (N_{new} - N_{safe})(t_D + H^*) \quad . \qquad (2.5)$$

The radial distribution of bubble nuclei has been found to follow a decaying exponential function (Fig. 3) [15] in several *in vitro* studies [5-7,10,13-15], and it is reasonable to assume that a similar distribution exists *in vivo*. The number of bubbles formed is [

$$N_{safe} = N_o \exp(-\beta_o S r_o / 2kT) \qquad (2.6)$$

for the original safe-ascent criterion and

$$N_{new} = N_o \exp(-\beta_o S r_o^{new} / 2kT) \qquad (2.7)$$

for the new augmented supersaturation, where N_o is a normalization constant, $\beta_o = 2(\gamma_C - \gamma)/r_o$ is determined from the model parameters, S is the effective surface area of one surfactant skin molecule *in situ*, r_o^{new} is the size of the smallest nucleus that contributes to the new bubble number, k is the Boltzmann constant, and T is the absolute body

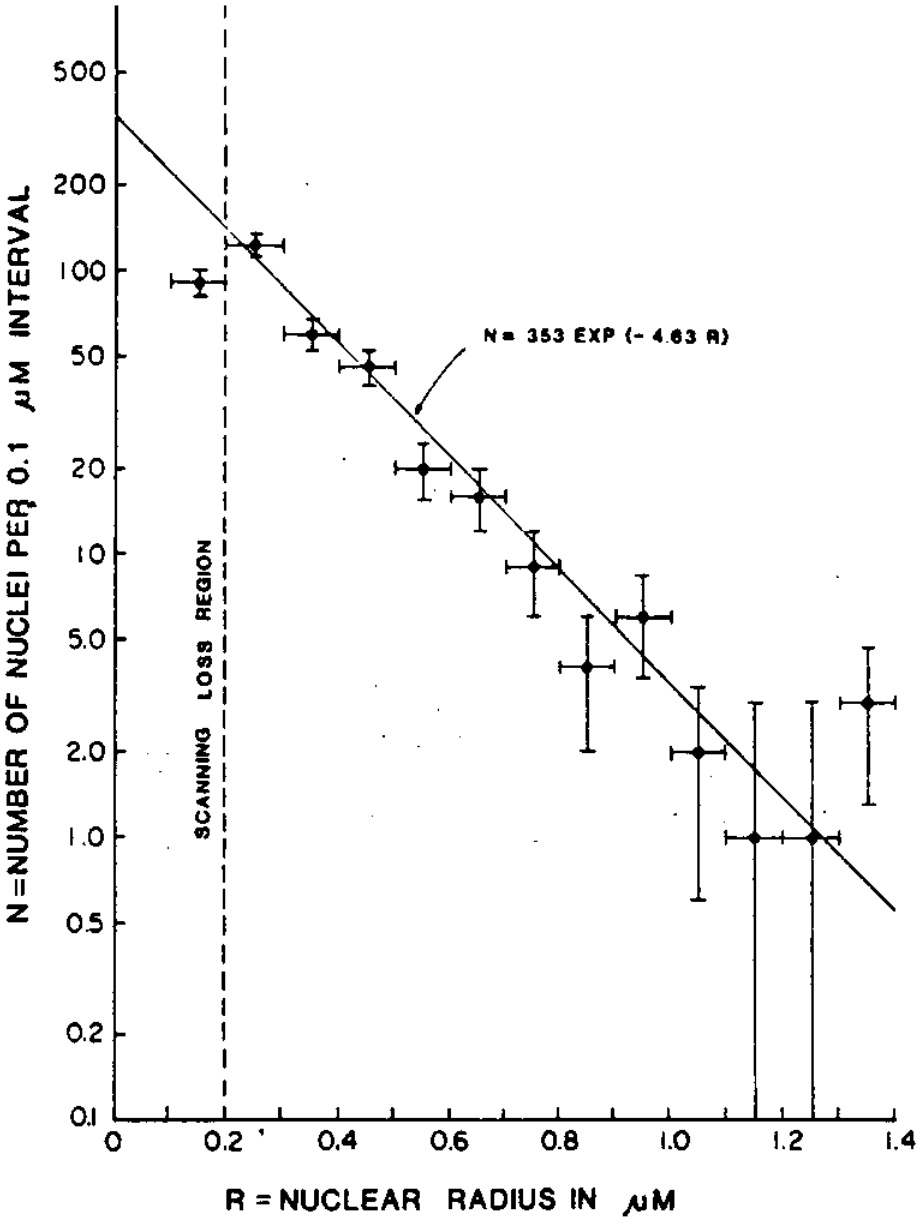

Fig. 3 - Differential radial distribution of gas cavitation nuclei in agarose gelatin. Above 0.2 μm, the points can be described by a decaying exponential. Below 0.2 μm, the microscope scanning efficiency deteriorates rapidly, and data in this region should be disregarded.

temperature. The difference in the bubble numbers can then be written

$$N_{new} - N_{safe} = N_o[\exp(-\beta_o Sr_o^{new}/2kT) - \exp(-\beta_o Sr_o/2kT)]. \quad (2.8)$$

If the exponential arguments are small, this simplifies to

$$N_{new} - N_{safe} \simeq N_o(\beta_o Sr_o^{new}/2kT)(1 - r_o^{new}/r_o) . \quad (2.9)$$

The last approximation is questionable, since the values of the model parameters are neither fixed nor known. If the approximation is not valid, the bubble numbers would simply correspond to a linear nuclear size distribution rather than the linear (small exponent) regime of an exponential distribution.

Eqs. (1.4) and (1.5) can be combined to give

$$P_{ss}^{safe} = 2\gamma(\gamma_C - \gamma)/\gamma_C r_o + (\gamma/\gamma_C)P_{crush} \quad (2.10)$$

and

$$P_{ss}^{new} = 2\gamma(\gamma_C - \gamma)/\gamma_C r_o^{new} + (\gamma/\gamma_C)P_{crush} . \quad (2.11)$$

Although Eq. (1.5) applies strictly only to the permeable regime, it varies little (less than 3%) when compared to the impermeable cubic equation at the maximum P_{crush} (largest deviation) encountered. It is therefore reasonable to use Eqs. (2.10) and (2.11) to simplify Eq. (2.9). The corresponding radii are

$$r_o = 2\gamma(\gamma_C - \gamma)/\{\gamma_C[P_{ss}^{safe} - P_{crush}(\gamma/\gamma_C)]\} \quad (2.12)$$

and

$$r_o^{new} = 2\gamma(\gamma_C - \gamma)/\{\gamma_C[P_{ss}^{new} - P_{crush}(\gamma/\gamma_C)]\} . \quad (2.13)$$

Inserting these results into Eq. (2.9), we obtain

$$N_{new} - N_{safe} \simeq \frac{[\beta_o N_o S r_o / 2kT](P_{ss}^{new} - P_{ss}^{safe})}{P_{ss}^{new} - (\gamma/\gamma_C)P_{crush}} \ . \tag{2.14}$$

The new supersaturation given by Eq. (2.5) is

$$P_{ss}^{new} \simeq \frac{2\chi V_C kT\,[P_{ss}^{new} - (\gamma/\gamma_C)P_{crush}]}{N_o \beta_o S r_o (t_D + H^*)(P_{ss}^{new} - P_{ss}^{safe})} \ , \tag{2.15}$$

which can be expressed in the standard quadratic form

$$(P_{ss}^{new})^2 - b(P_{ss}^{new}) + c = 0 \ , \tag{2.16}$$

where

$$b = P_{ss}^{safe} + \alpha/(t_D + H^*) \ , \tag{2.17}$$

$$c = (\gamma/\gamma_C)P_{crush}[\alpha/(t_D + H^*)] \ , \tag{2.18}$$

and

$$\alpha = 2\chi V_C kT/N_o \beta_o S r_o = \chi V_C kT/N_o(\gamma_C - \gamma)S \ . \tag{2.19}$$

Quantities such as χ, S, V_C, N_o, N_{new}, and N_{safe} are, of course, absorbed into the third free parameter α and are never explicitly determined. The solution for the new allowed supersaturation is

$$P_{ss}^{new} = [b + (b^2 - 4c)^{1/2}]/2 \ , \tag{2.20}$$

which has been inserted directly into the computer program. However, since t_D depends on P_{ss}^{new}, Eq. (2.20) must be iterated to convergence, evident when two successive calculations give virtually the same total decompression time t_D.

B. TISSUE TENSION

The allowed tissue supersaturation provided by Eq. (2.20) must be converted to an allowed depth before a decompression step can be made. So long as the difference between the tissue tension τ and the ambient pressure P_{amb} does not exceed that allowed supersaturation, the critical volume of free gas will not be exceeded. The constraining relationship is therefore

$$\tau(t) - P_{amb}(t) \leq P_{ss}^{new} \quad , \tag{2.21}$$

where the equals sign is adopted to minimize the total decompression time. If the time scale for equilibration of the body with the breathing gas is short compared to the rate of change of depth, the ambient pressure will correspond to the current depth of sea water. The ascent criterion is then

$$D_a(t) = \tau(t) - P_{ss}^{new} \quad , \tag{2.22}$$

in which D_a is the allowed depth. Once the tissue tension is known as a function of time, Eq. (2.22) will provide the exact depth requirements. However, since ascents are normally made in stages rather than continuously, the computer program adjusts D_a in even increments (of 10 fsw) and solves for the elapsed time instead.

The tissue tension calculation is based upon a perfusion-limited rate equation [31],

$$\frac{d\tau(t)}{dt} = k[P_a(t) - \tau(t)] \quad , \tag{2.23}$$

where $k = (\ln 2)/H$ and H is the tissue half-time. The partial pressure

P_a of a single inert gas in the breathing mixture is assumed to be proportional to the ambient pressure P_{amb}, where F is the constant of proportionality. The fraction of nitrogen is fixed at F = 0.79 in all the air-table calculations. Oxygen, carbon dioxide, and water vapor will be taken into account shortly. The rate equation is then

$$\frac{d\tau(t)}{dt} = k[FP_{amb} - \tau(t)]$$

or

$$\frac{d\tau(t)}{dt} + k\,\tau(t) = kFP_{amb} \quad . \tag{2.24}$$

The homogeneous solution to Eq. (2.24) is of the form

$$\tau(t) = Ae^{-kt} \quad . \tag{2.25}$$

The change in the total ambient pressure during any linear (constant velocity) depth excursion from an initial pressure P_o is given by

$$P_{amb} = P_o + vt \quad , \tag{2.26}$$

where v has the units of fsw/min and t is the duration of the excursion in minutes. Inserting Eq. (2.26) into Eq. (2.24), we find that the particular solution to the rate equation is

$$\tau(t) = F(P_o + vt - v/k) \quad . \tag{2.27}$$

The complete solution is the sum of the homogeneous and particular solutions, or

$$\tau(t) = Ae^{-kt} + F(P_o + vt - v/k) \quad . \tag{2.28}$$

To evaluate the constant A, we assume that the excursion begins at time $t = 0$ and at depth $P_{amb} = P_o$. This yields

$$\tau(0) = A + F(P_o - v/k)$$

or

$$A = \tau(0) - F(P_o - v/k) \quad . \tag{2.29}$$

Using the above equations, we may insert any arbitrary starting depth P_o with its corresponding tissue tension $\tau(0)$ and calculate the tissue tension as a function of time, even if there is no excursion (constant depth). To describe the various bodily tissue types, fixed half-times for some fifteen tissue compartments have been included (Fig. 1), ranging (for nitrogen) from one minute to twelve hours [31,32,41,51-55]. They are intended to span the full range of diving experience, from no-stop decompressions to saturation dives. Of these tissue half-times, one will be found to yield the greatest tension via Eq. (2.28) and is thus said to be "controlling" the ascent through Eq. (2.22). The half-times of the controlling tissues tend toward larger values as the elapsed decompression time increases.

Oxygen, carbon dioxide, and water vapor have been treated as a group labeled "active" gases. The details of their treatment have already been published [30], so only a brief statement is presented here. The contribution of the active gases to the inert gas tension can be found by subtracting the "oxygen window" (Fig. 4) from the inspired oxygen pressure. The oxygen window calculation is based upon the

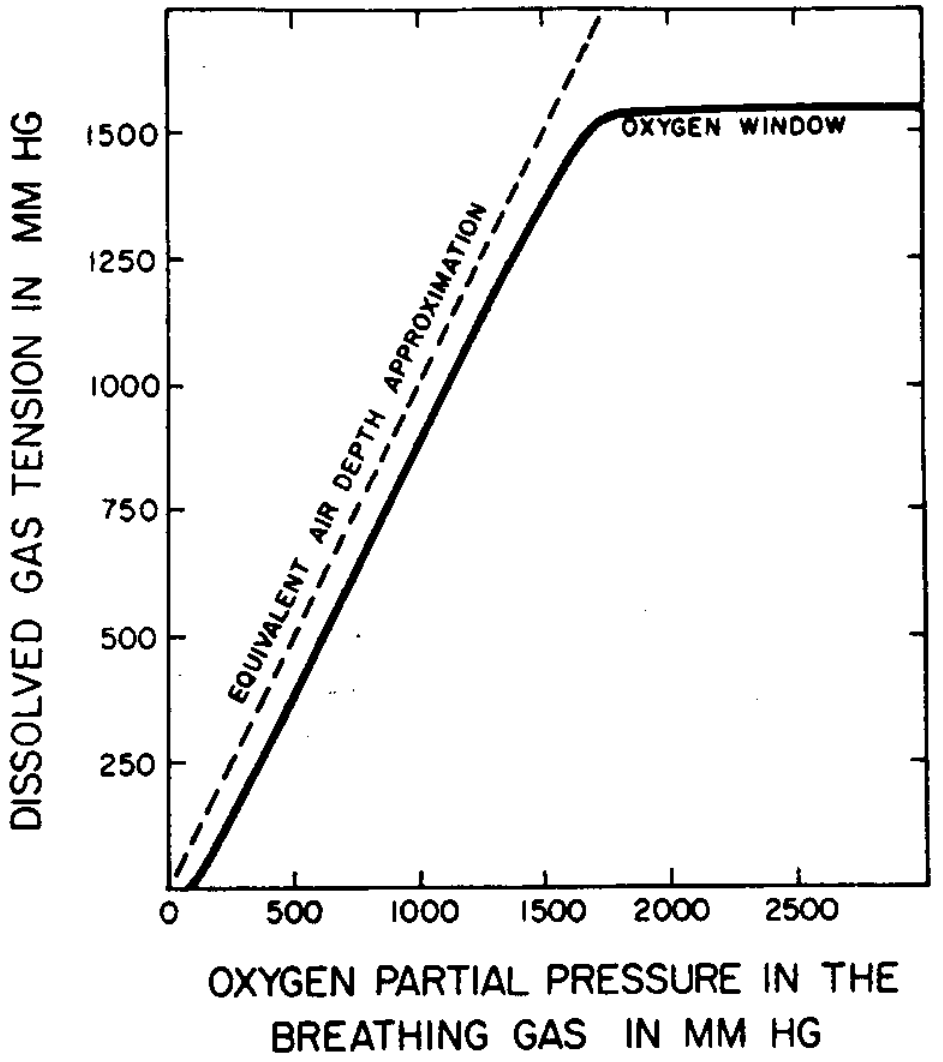

Fig. 4 - Plot of dissolved gas tension versus oxygen partial pressure. The equivalent-air-depth approximation is useful for oxygen partial pressures below 1500 mm Hg.

inhalation of "dry" air containing no carbon dioxide, using the normal values of 47 mm Hg for water vapor pressure and 40 mm Hg for the arterial carbon dioxide pressure. A remarkable fact is that the result of the subtraction is very nearly constant at 102 mm Hg until the oxygen partial pressure reaches about 1500 mm Hg. The active-gas contribution to the inert gas tension has therefore been set at 4.43 fsw (102 mm Hg) for O_2 pressures below 1500 mm Hg, and at 4.43 fsw plus the excess oxygen partial pressure (inspired pressure less 1500 mm Hg) for higher O_2 pressures. For O_2 partial pressures above 360 mm Hg, care must be exercised to guard against oxygen toxicity.

C. NUCLEAR REGENERATION

As illustrated in Fig. 2 [6], samples of knox gelatin display increased resistance to bubble formation following the rapid application of a crushing pressure [5-7]. The same effect occurs <u>in vivo</u>, as can be seen in Figs. 5 [11] and 6 [30]. The larger the exposure pressure, the fewer the bubbles that form with the same allowed supersaturation during decompression. The varying-permeability model dictates that bubble nuclei are "crushed" by the mechanical strength of the initial compression and that the number of nuclei larger than the critical radius decreases. Surfactant molecules are forced out of the nuclear skin into solution, perhaps into a "reservoir" just outside, where they remain available to retake their old positions.

The equilibrium exponential radial distribution of bubble nuclei has been derived from statistical-mechanical considerations, and it has been shown theoretically that a nuclear population, once crushed, is

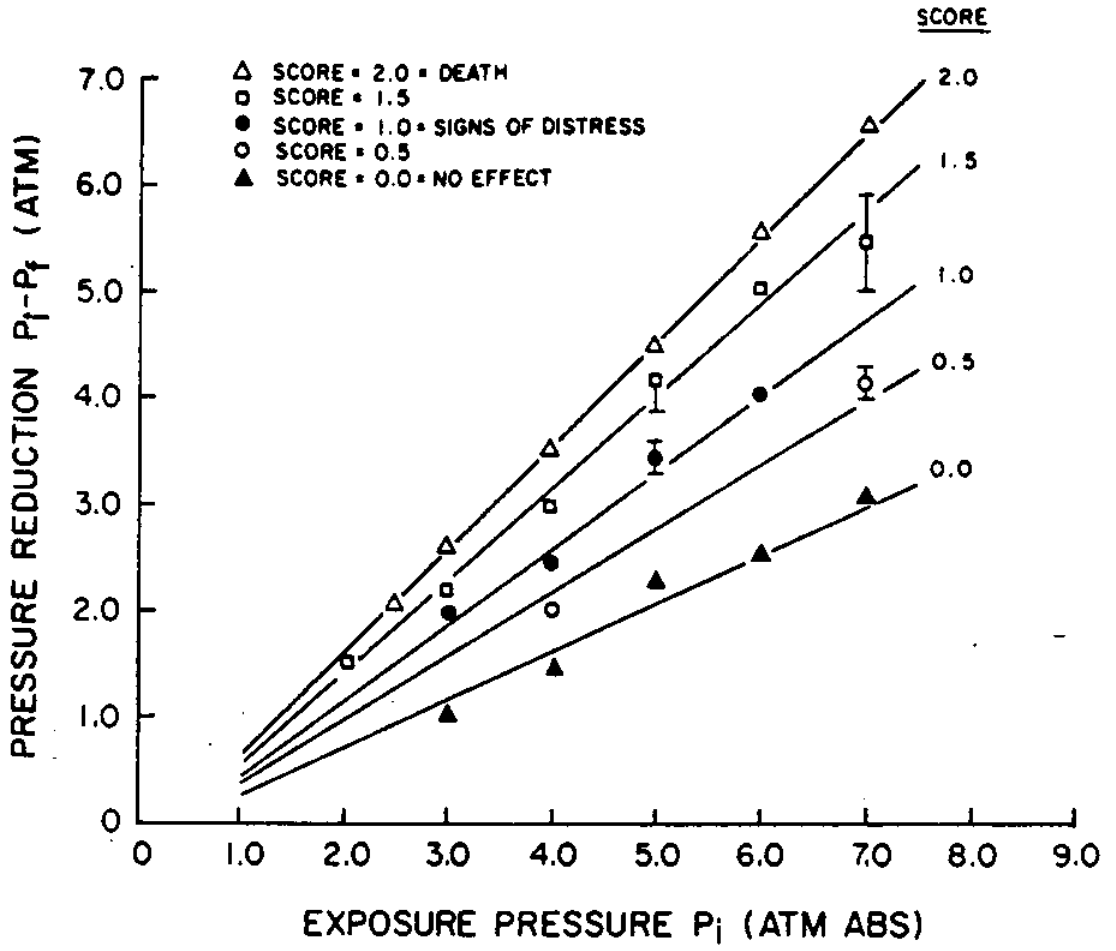

Fig. 5 - Limits of pressure reduction versus exposure pressure for fingerling salmon. The respective VPM predictions are straight lines.

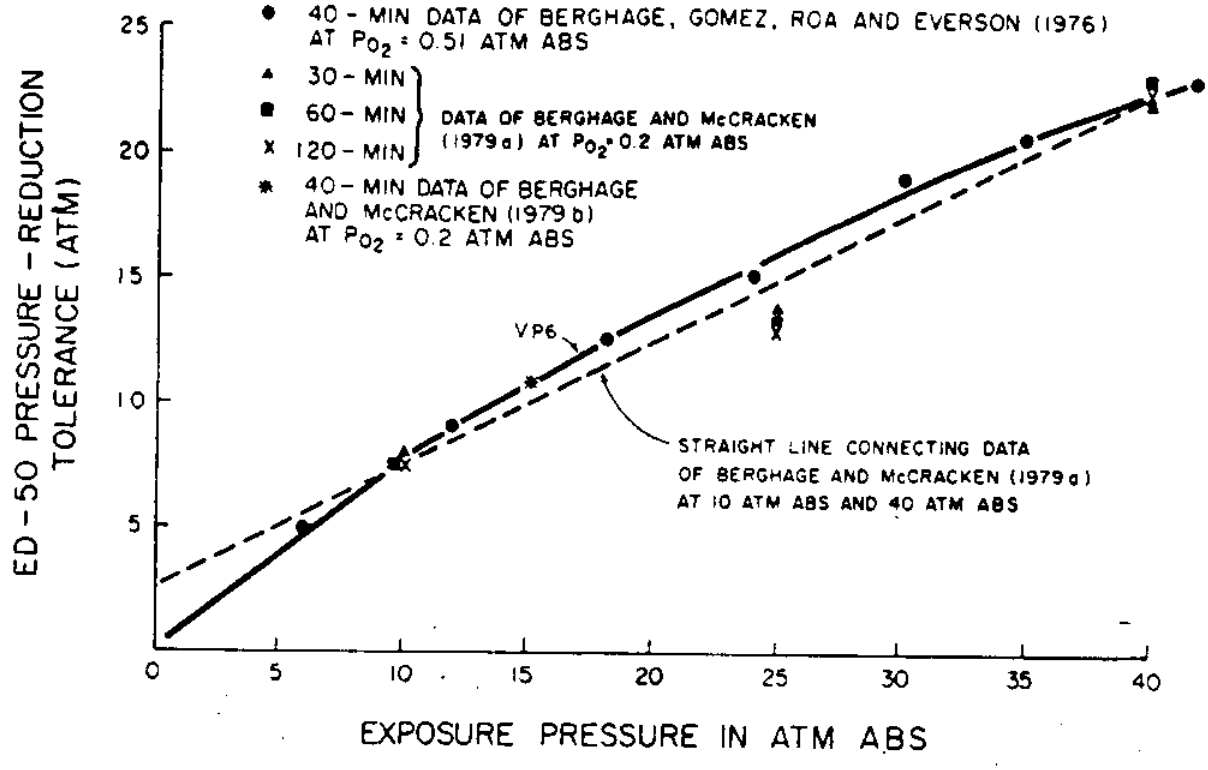

Fig. 6 - Compilation of pressure-reduction tolerances versus exposure pressure for albino rats. ED-50 is the pressure reduction needed to produce decompression sickness in 50% of the animals. The solid curve summarizes the VPM predictions. Note that pressure-reduction tolerance increases significantly with exposure pressure.

capable of stochastically restoring that distribution [16]. The time constant for such "nuclear regeneration" is assumed to be comparatively long, ranging from several hours to days or weeks. One implication is that divers might become "acclimated" by diving regularly and depleting the nuclear population, only to contract the bends when returning after a leave of absence, since this population has regenerated and decreased their decompression tolerance. Another situation is that of lengthy saturation dives, such as the Tektite 14-day exposure at 100 fsw. Any beneficial effect provided by crushing may have been "forgotten" prior to returning to the surface. In order to accommodate the phenomenon of nuclear regeneration, the computer program has been designed to track nuclear growth continuously following the initial compression. This is accomplished by allowing the minimum nuclear radius r_m to evolve gradually back into the original critical radius r_o. The time-dependence is approximated by the exponential relation

$$r_m(t) = r_m(0) + \{1 - \exp(-t/\tau_r)\} [\, r_o - r_m(0) \,] \quad . \qquad (2.30)$$

The time constant τ_r is the fourth and last of the free parameters used to calculate the VPM tables. It may be argued that some of the model constants, such as the impermeability threshold or the tissue compartment half-times, have been arbitrarily selected and therefore should have been included in our list. However, each of those constants was presumably fixed prior to the application of the model to the construction of diving tables, whereas the four variable parameters were optimized to "tune" the output to the body of available data on safe ascents. No variable or constant (other than the excursion profiles)

needs to be added or changed to calculate any of the literally thousands of VPM air and helium schedules represented in this work, or any new schedule within the same range. It is the physical model which facilitates our table calculations, not the inclusion of "hidden" parameters, and it is a notable feature of the nucleation approach—evident already in this naive formulation—that the usual proliferation of free pa meters (e.g., M-values) can be avoided.

Very little has bee said about the physiological processes which presumably underlie the mathematical equations in this chapter. Obviously, oxygen and carbon dioxide were taken into account, and typical ranges for the tissue half-times were assumed. However, no distinction was made between "fatty, loose tissue" and "watery, tight tissue" [29], nor was it explicitly stated where the bubbles form or how they grow, multiply, or are transported. Finally, nothing was said about such factors as solubility, diffusion versus perfusion, tissue deformation pressure, or tissue-specific differences in surface tension. Since all of the omitted items are not well understood, at least <u>in vivo</u>, the main effect of attempting to take any of them into account would be to increase the number of free parameters. For example, this number could be doubled simply by assuming a different set of nucleation parameter values for aqueous and lipid constituents.

REFERENCES

1. Yount, D.E. and R.H. Strauss. 1977. Decompression sickness. American Scientist 65(5):598-604.

2. Strauss, R.H. 1974. Bubble formation in gelatin: implications for prevention of decompression sickness. Undersea Biomed. Res. 1(2):169-174.

3. Strauss, R.H. and T.D. Kunkle. 1974. Isobaric bubble growth: a consequence of altering atmospheric gas. Science 186:443-444.

4. Kunkle, T.D. and D.E. Yount. 1975. Gas nucleation in gelatin. In: Proc. Sixth Symp. Underwater Physiol., ed. M.B. Kent, pp. 459-467. Bethesda: Federation of American Societies for Experimental Biology.

5. Yount, D.E. and R.H. Strauss. 1976. Bubble formation in gelatin: a model for decompression sickness. J. Appl. Phys. 47(11): 5081-5089.

6. Yount, D.E., C.M. Yeung, and F.W. Ingle. 1977. Determination of the radii of gas cavitation nuclei by filtering gelatin. J. Acoust. Soc. Am. 65(6):1440-1450.

7. Yount, D.E. and C.M. Yeung. 1981. Bubble formation in supersaturated gelatin: a further investigation of gas cavitation nuclei. J. Acoust. Soc. Am. 69(3):702-708.

8. D'Arrigo, J.S. 1978. Improved method for studying the surface chemistry of bubble formation. Aviat. Space Environ. Med. 49(2):358-361.

9. Paganelli, C.V., R.H. Strauss, and D.E. Yount. 1977. Bubble formation within decompressed hen's eggs. Aviat. Space Environ. Med. 48(1):48-49.

10. Yount, D.E. 1979. Skins of varying permeability: a stabilization mechanism for gas cavitation nuclei. J. Acoust. Soc. Am. 65(6):1429-1439.

11. Yount, D.E. 1979. Application of a bubble formation model to decompression sickness in rats and humans. Aviat. Space Environ. Med. 50(1):44-50.

12. Yount, D.E. 1981. Application of a bubble formation model to decompression sickness in fingerling salmon. Undersea Biomed. Res. 8(4):199-208.

13. Yount, D.E., E.W. Gillary, and D.C. Hoffman. 1982. A microscopic study of gas cavitation nuclei. In: Cavitation and Polyphase Flow Forum, ed. J.W. Hoyt, pp. 6–8. New York: The American Society of Mechanical Engineers.

14. Yount, D.E., E.W. Gillary, and D.C. Hoffman. 1984. Microscopic study of bubble formation nuclei. In: Proc. Eighth Symp. Underwater Physiol., ed. A.J. Bachrach and M.M. Matzen, pp. 119-130. Bethesda, Md: Undersea Medical Society, Inc.

15. Yount, D.E., E.W. Gillary, and D.C. Hoffman. 1984. A microscopic investigation of bubble formation nuclei. J. Acoust. Soc. Am. 76(5):1511-1521.

16. Yount, D.E. 1982. On the evolution, generation, and regeneration of gas cavitation nuclei. J. Acoust. Soc. Am. 71(6):1473-1481.

17. Yount, D.E. and D.C. Hoffman. 1983. Decompression theory: a dynamic critical-volume hypothesis. In: Proc. Eighth Symp. Underwater Physiol., ed. A.J. Bachrach and M.M. Matzen, pp. 131-146. Bethesda, Md: Undersea Medical Society, Inc.

18. Yount, D.E. and D.C. Hoffman. 1983. On the use of a cavitation model to calculate diving tables. In: Cavitation and Multiphase Flow Forum, ed. J.W. Hoyt, pp. 65–68. New York: The American Society of Mechanical Engineers.

19. U.S. Department of the Navy. 1977. U.S. Navy Diving Manual (NAVSHIPS 0994-LP-001-9010). Washington: U.S. Government Printing Office.

20. Royal Naval Physiological Laboratory. 1968. Air Diving Tables. Alverstoke, Hants. London: Her Majesty's Stationary Office.

21. Landau, L.D. and E.M. Lifshitz. 1938. Statistical Physics, pp. 225-228. Oxford: Oxford University Press.

22. Frenkel, J. 1955. The kinetic theory of liquids, chap. VII New York: Dover Publications.

23. Harvey, E.N. et al. 1944. Bubble formation in animals, I. Physical factors. J. Cell. Comp. Physiol. 24:1-22.

24. Pease, D.C. and L.R. Blinks. 1947. Cavitation from solid surfaces in the absence of gas nuclei. J. Phys. Col. Chem. 51:556-567.

25. Yount, D.E. et al. 1977. Stabilization of gas cavitation nuclei by surface-active compounds. Aviat. Space Environ. Med. 48(3):185-191.

26. Spencer, M.P. and S.D. Campbell. 1968. Development of bubbles in venous and arterial blood during hyperbaric decompression. Bull Mason Clinic 22:26-32.

27. Yount, D.E. 1983. A model for microbubble fission in surfactant solutions. J. Colloid Interface Sci. 91:349-360.

28. Albano, G. 1970. Principles and observations on the physiology of the scuba diver. Published in Italian in 1966 and translated for the Office of Naval Research, ONR Report DR0150.

29. Hennessey, T.R. and H.V. Hempleman. 1977. An examination of the critical released gas volume concept of decompression sickness. Proc. R. Soc. Lond. Biol. 197:299-313.

30. Yount, D.E. and D.A. Lally. 1980. On the use of oxygen to facilitate decompression. Aviat. Space Environ. Med. 51(6): 544-550.

31. Flynn, E.T., et al. 1981. Diving Medical Officer Student Guide, Course A-6A-0010. Naval Diving and Salvage Training Center, Panama City, FL 32407.

32. Beckman, E.L. 1976. Recommendations for Improved Air Decompression Schedules for Commercial Diving. UNIHI-SEAGRANT-TR-76-02. University of Hawaii Sea Grant College Program, Honolulu.

33. Hills, B.A. 1966. A thermodynamic and kinetic approach to decompression sickness. Ph.D. dissertation, Department of Chemical Engineering, University of Adelaide, Australia.

34. Leitch, D.R. and E.E.P. Barnard. 1982. Observations on no-stop and repetitive air and oxynitrogen diving. Undersea Biomed. Res. 9:113-129.

35. Beckman, E.L. and E.M. Smith. 1972. Tektite II: Medical supervision of the scientists in the sea. Texas Reports on Biol. and Med. 30:155-169.

36. Hempleman, H.V. 1969. Decompression theory: British practice. In: The physiology and medicine of diving and compressed air work. Eds. Bennett, P.B. and D.H. Elliott, pp. 331-347. Baltimore: Williams & Wilkins.

37. Kidd, D.J., R.A. Stubbs, and R.S. Weaver. 1971. Comparative approaches to prophylactic decompression. In: Proc. Fourth Symp. Underwater Physiol., ed. C.J. Lambertsen, pp. 167-177. New York: Academic Press.

38. Gray, J.S. 1944. Aeroembolism induced by exercise in cadets at 23,000 feet. Committee on Aviation Medicine Report 260. Washington, D.C.: United States National Research Council.

39. Beard, S.E., T.H. Allen, R.G. McIver, and R.W. Bancroft. 1967. Comparison of helium and nitrogen in production of bends in simulated orbital flights. Aerospace Med. 38(4):331-337.

40. Bennett, P.B. and A.J. Hayward. 1968. Relative decompression sickness hazards in rats of neon and other inert gases. Aerospace Med. 39(3):301-302.

41. Buhlmann, A.A. 1984. Decompression—Decompression Sickness. New York: Springer-Verlag. (Available through: Best Publishing Company, P.O. Box 1978, San Pedro, CA 90732).

42. Yount, D.E. 1978. Responses to the twelve assumptions presently used for calculating decompression schedules. In: Decompression Theory, the Seventeenth Undersea Medical Society Workshop, pp. 143-160. Bethesda, Md.: Undersea Medical Society, Inc.

43. Behnke, A.R. 1971. The Harry G. Armstrong Lecture. Decompression sickness: advances and interpretations. Aerospace Med. 42(3):255-267.

44. Gersh, I. and H.R. Catchpole. 1951. Decompression sickness: physical factors and pathologic consequences. In: Decompression Sickness, J.F. Fulton, Ed. Philadelphia: W.B. Saunders.

45. Blank, M. 1979. Monolayer permeability. Progress in Surface and Membrane Science 13:87-139.

46. Kunkle, T.D. 1979. Bubble nucleation in supersaturated fluids. Sea Grant Technical Report UNIHI-SEAGRANT-TR-80-1. NOAA Office of Sea Grant, U.S. Department of Commerce.

47. Adamson, A.W. 1976. The physical chemistry of surfaces, 3rd ed., Chapters II and III. New York: John Wiley & Sons.

48. Gaines, G.L. 1966. Insoluble monolayers at liquid-gas interfaces, Chapter IV, Sec. III. New York: John Wiley & Sons, Inc.

49. Ries, H.E., Jr. and W.A. Kimball. 1957. Proceedings of the Second International Congress of Surface Activity, Vol. I, pp. 75-84.

50. Tanford, C. 1980. The hydrophobic effect: formation of micelles and biological membranes, 2nd Ed. New York: John Wiley & Sons.

51. Lambertsen, C.J. and H. Bardin. 1973. Decompression from acute and chronic exposure to high nitrogen pressure. Aerospace Med. 44(7):834-836.

52. Buhlmann, A.A., P. Frei, and H. Keller. 1966. Saturation and desaturation with N_2 and He at 4 atm. J. Appl. Physiol. 23(4):458–462.

53. Krekler, H., G. von Nieding, K. Muysers, P. Cabarrou, and D. Fust. 1973. Washout of inert gases following hyperbaric exposure. Aerospace Med. 44(5):505–507.

54. Schreiner, H.R. and P.L. Kelley. 1966. Computation methods for decompression from deep dives. Proc. Third Symp. Underwater Physiol., C.J. Lambertsen, Ed., pp. 275–299. Baltimore: Williams and Wilkins.

55. Schilling, C.W., M.F. Werts, and N.R. Schandelmeier, Eds. 1976. The underwater handbook: a guide to physiology and performance for the engineer. New York: Plenum Press.

56. Workman, R.D. and J.L. Reynolds. 1965. Adaptation of helium-oxygen to mixed-gas SCUBA. U.S. Navy Experimental Diving Unit Research Report 1-65.

57. Workman, R.D. 1965. Calculation of decompression schedules for nitrogen-oxygen and helium-oxygen dives. U.S. Navy Experimental Diving Unit Report 6-65.

58. Molumphy, G.G. 1950. Computation of helium-oxygen decompression tables. U.S. Navy Experimental Diving Unit Report 7-50.

59. Molumphy, G.G. 1950. Helium-oxygen decompression tables. U.S. Navy Experimental Diving Unit Report 8-50.

60. Hills, B.A. 1977. Decompression sickness, Volume 1, Chapter 7. New York: John Wiley & Sons.

61. Hempleman, H.V. 1967. Decompression procedures for deep, open sea operations. In: Proc. Third Symp. Underwater Physiol., C.J. Lambertsen, Ed., pp. 255–266. Baltimore: Williams & Wilkins.

62. Elliott, D.H. 1969. Some factors in the evaluation of oxy-helium decompression schedules. Aerospace Med. 40(2):129–132.

63. Bornmann, R.C. 1966. Decompression after saturation diving. In: Proc. Third Symp. Underwater Physiol., C.J. Lambertsen, Ed., pp. 255–266. Baltimore: Williams & Wilkins.